AFWAL-TR-86-3003
Volume V

(2)

AD-A175 111

ASSESSMENT OF DAMAGE TOLERANCE REQUIREMENTS AND ANALYSES - TASKS VI, VII, VIII REPORT

Volume V - Assessment and Recommendations

M. LEVY

Fairchild Industries
Fairchild Republic Company
Farmingdale, N.Y. 11735

SEPTEMBER 1986

Final Technical Report for Period September 1982 - November 1985

FLIGHT DYNAMICS LABORATORY
AIR FORCE WRIGHT AERONAUTICAL LABORATORIES
AIR FORCE SYSTEMS COMMAND
WRIGHT-PATTERSON AIR FORCE BASE, OHIO 45433-6553

86 12 15 085

UNCLASSIFIED
SECURITY CLASSIFICATION OF THIS PAGE

REPORT DOCUMENTATION PAGE

1a. REPORT SECURITY CLASSIFICATION: Unclassified	1b. RESTRICTIVE MARKINGS: A175111
2a. SECURITY CLASSIFICATION AUTHORITY	3. DISTRIBUTION/AVAILABILITY OF REPORT: Approved for public release; distribution unlimited.
2b. DECLASSIFICATION/DOWNGRADING SCHEDULE	
4. PERFORMING ORGANIZATION REPORT NUMBER(S)	5. MONITORING ORGANIZATION REPORT NUMBER(S): AFWAL-TR-86-3003, Vol. V
6a. NAME OF PERFORMING ORGANIZATION: Fairchild Industries, Fairchild Republic Co. / 6b. OFFICE SYMBOL (If applicable)	7a. NAME OF MONITORING ORGANIZATION: Flight Dynamics Laboratory (AFWAL/FIBEC)
6c. ADDRESS (City, State, and ZIP Code): Farmingdale, N.Y. 11735	7b. ADDRESS (City, State, and ZIP Code): Wright-Patterson Air Force Base Ohio, 45433-6553
8a. NAME OF FUNDING/SPONSORING ORGANIZATION: AFWAL / 8b. OFFICE SYMBOL (If applicable): FIBEC	9. PROCUREMENT INSTRUMENT IDENTIFICATION NUMBER: F33615-82-C-3215
8c. ADDRESS (City, State, and ZIP Code): Wright-Patterson AFB OH 45433-6553	10. SOURCE OF FUNDING NUMBERS: PROGRAM ELEMENT NO. 62201F; PROJECT NO. 2401; TASK NO. 01; WORK UNIT ACCESSION NO. 61

11. TITLE (Include Security Classification)
Assessment of Damage Tolerance Requirements and Analyses—TASKS VI, VII, VIII REPORT
Volume V: Assessment and Recommendations

12. PERSONAL AUTHOR(S)
Meir Levy

13a. TYPE OF REPORT	13b. TIME COVERED	14. DATE OF REPORT (Year, Month, Day)	15. PAGE COUNT
Final	FROM Sept 82 TO Nov 85	1986/September	27

16. SUPPLEMENTARY NOTATION

17. COSATI CODES			18. SUBJECT TERMS (Continue on reverse if necessary and identify by block number)
FIELD	GROUP	SUB-GROUP	Damage Tolerance, MIL-A-83444, Crack Growth, Crack Initiation, Lap-Joint Specimens, Stringer Reinforced Specimens.
13	13		
13	05		

19. ABSTRACT (Continue on reverse if necessary and identify by block number)

A structural test program of typical aircraft structural configuration was conducted to assess the current Air Force damage tolerance design requirements defined in MIL-A-83444. The specimens, made of 2024-T3XX and 7075-T6XX, were subjected to randomized flight-by-flight spectra, representative of fighter/trainer and bomber/cargo type loading spectra, respectively, and to constant amplitude loading spectrum. A total of 72 specimens were tested. The test results were correlated with analytical predictions using the crack growth method and combined method. As a result of this study, recommendation is provided to the validity of MIL-A-83444, to develop guidelines for selection of critical crack locations, and to assess the state-of-the-art analytical capabilities in predicting crack growth and crack initiaiton time.

This volume, Volume V, of a five-volume report presents the assessment and recommendations pertaining to the current damage tolerance design requirements and analyses based on the analyses and testing done under this contract.

20. DISTRIBUTION/AVAILABILITY OF ABSTRACT: ☐ UNCLASSIFIED/UNLIMITED ☐ SAME AS RPT ☐ DTIC USERS	21. ABSTRACT SECURITY CLASSIFICATION: Unclassified
22a. NAME OF RESPONSIBLE INDIVIDUAL: Lt. christopher Mazur	22b. TELEPHONE (Include Area Code): (513)255-6104 / 22c. OFFICE SYMBOL: AFWAL/FIBEC

DD FORM 1473, 84 MAR — 83 APR edition may be used until exhausted. All other editions are obsolete.

SECURITY CLASSIFICATION OF THIS PAGE
UNCLASSIFIED

FOREWORD

This is Volume V of the five-volume report entitled "Assessment of Damage Tolerance Requirements and Analyses," Contract No. F33615-82-C-3215. This program has been administrated by the Flight Dynamics Laboratory, Air Force Wright Aeronautical Laboratories, Air Force Systems Command, Wright Patterson Air Force Base, Ohio. James L. Rudd (AFWAL/FIBEC) was the Air Force Project Engineer through December 1985. Subsequently, Mr Rudd was replaced by Lt Christopher Mazur. Albert Kuo was FRC Program Manager and Principal Investigator through March 1985. Subsequently, Meir Levy assumed the responsibility for the completion of the program. The structural test program has been performed at the University of Dayton Research Lab under the supervision of George Roth.

The title on the front cover is correct for this report.
Per Ms. Martha Kline, AFWAL/IMST

TABLE OF CONTENTS

LIST OF TABLES

LIST OF FIGURES

1.0 INTRODUCTION

Eight major tasks listed below have been planned to achieve the program objectives. Namely, (a) assessing the validity of, and recommending improvements to MIL-A-83444, (b) developing guidelines for identifying the most critical initial primary damage locations for typical aircraft structures, and (c) assessing and improving the state-of-the-art analytical methods to satisfy the requirements of MIL-A-83444.

Task I:	Analytical Methods
Task II:	Basic Tests
Task III:	Analytical Predictions
Task IV:	Structural Tests
Task V:	Analytical/Experimental Correlations
Task VI:	Assessment of and Recommended Improvements to MIL-A-83444
Task VII:	Guidelines for Selecting Most Critical Initial Primary Damage Location
Task VIII:	Assessment of and Improvements to Damage Tolerance Analyses

This report is Volume V of a five-volume report. The material presented in this volume provides assessment and recommendations as described in Tasks VI, VII and VIII. The other four volumes include:

Volume I:	Executive Summary
Volume II:	Analytical Methods
Volume III:	Analytical Predictions and Correlations
Volume IV:	Raw Test Data

Volume I contains an Executive Summary of the entire program including the Basic Test Program for material allowables, test results of the Structural Test Program and Analytical Predictions. It also contains a summary of the Analytical Formulation derived during Task I.

Volume II presents the Analytical Methodology derived during Task I of the Program, including crack growth and crack initiation techniques, and results of Finite Element Modeling of stress intensity factors.

Volume III presents Analytical to Experimental Correlation of seventy-two (72) Structural Test Specimens performed during Task IV of the Program.

Volume IV presents the Raw Test Data obtained during the Basic Test, and the Structural Test Programs.

In addition, a user manual of the DAMGRO Computer Program has been released.

2.0 DAMAGE TOLERANCE DESIGN REQUIREMENT ASSESSMENT

The requirements for initial flaw assumptions of a primary airframe structure are defined in the Military Specification MIL-A-83444. Utilizing these assumptions, the life of a structural part subjected to flight-by-flight loading spectrum can be determined. The assumptions include a primary initial flaw at the most critical area of an element, and a secondary flaw at a specified adjacent location. The size and the shape of the primary, and the secondary flaws are also defined in the MIL-A-83444. The crack growth analysis usually does not take into consideration the beneficial effect of various geometrical constraints, such as fastener interference or bolt clamp-up. However, in some cases when verification of the beneficial effect exists, relaxation of the initial flaw requirements in MIL-A-83444 may be considered on a case-by-case basis. Typical initial flaw requirements at fastener holes are shown in Figure 2.1. It includes the initial flaw of 0.050 inch, and a secondary flaw of 0.005 inch. The secondary flaw assumption often depends on the structural configuration of the part, and sometimes involves engineering judgement.

The test results obtained from 72 specimens which were subjected to randomized loading spectra, and to a constant amplitude loading spectrum, were used to make the conclusions and recommendations relative to the requirements in MIL-A-83444. Analytical Predictions were performed and correlated against the test results. The predictions were performed using two analytical methods; the crack growth method and the combined method (Ref. Vol. III). The crack growth method utilizes the existing fracture mechanics techniques to predict crack growth life. The combined method utilizes crack growth and crack initiation to predict the life of the element. In predicting crack initiation, the strain energy density ($S = 0.5\,(\sigma K)^2/E$) at the edge of a hole was used as a parameter in governing the crack initiation. The beneficial effects due to fastener interference, fastener clamp-up and faying surface sealant were evaluated to determine their beneficial effect on crack initiation, and subsequent growth (Ref. Vols. III and IV). Some of the parameters which account for the geometrical constraints were derived during Phase I of the program using simple Dog-Bone type specimens. Other parameters were obtained from the literature or using finite element models (Ref. Vol. II).

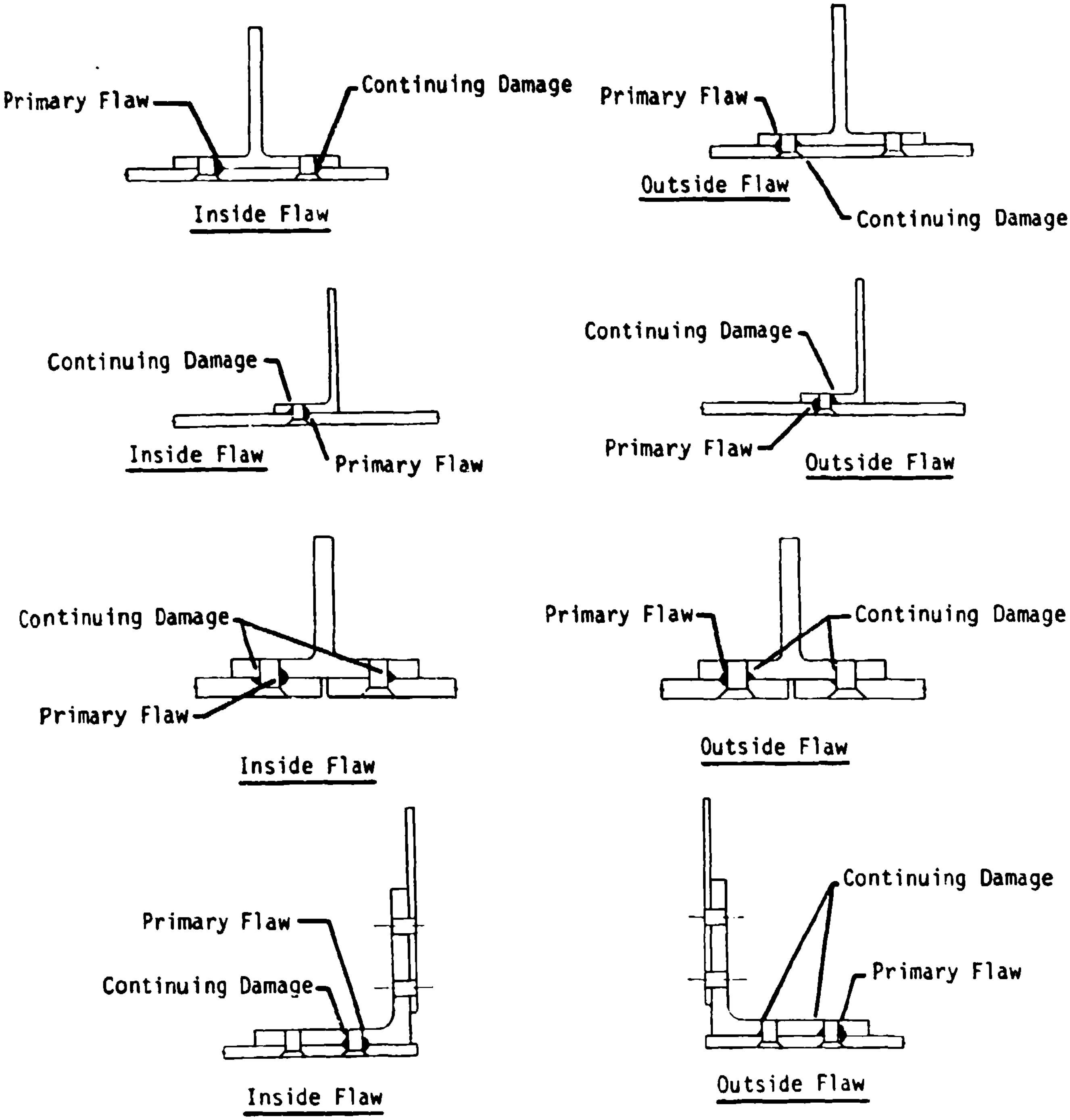

Figure 2.1. Initial Flaw Assumptions Consistent With MIL-A-83444

2.1 TEST RESULTS EVALUATION

The test results of 72 structural test specimens were examined to determine the extent of crack growth and crack initiation. Each representative group of specimens (Ref. Tables 2.1 and 2.2) were examined using NDI equipment to determine the site as well as the sequence of crack initiation. The specimens tested included single-shear and double-shear lap-joint specimens and stringer-reinforced specimens. The lap-joint specimens were intended to represent a chordwise structural joint such as wing-rib structure. The stringer-reinforced specimens were typical of wing panel configurations. The lap-joint specimens contained closely spaced rivets with high load transfer. This type of configuration is known to have an adverse effect on crack growth life and crack initiation.

The stringer-reinforced specimens included four (4) structural configurations;

a) Center tee-stringer with continuous skin,

b) Center L-stringer with continuous skin,

c) Edge L-stringer with continuous skin,

d) Center tee-stringer with split skin.

Each group of specimens contained two initial flaw configurations. One group contained an initial flaw with orientation facing the upstanding leg of the stringer, called an "inside flaw." The second group contained an initial flaw with orientation facing the free edge of the stringer, called an "outside flaw." All initial flaws were 0.050-inch corner cracks, and were initiated by means of saw-cut followed by application of constant amplitude loading.

The structural test specimens were subjected to a constant amplitude (C.A.) and to variable amplitude loading spectra. The two variable amplitude loading spectra included A-10A loading spectrum representative of fighter-trainer-type maneuver spectrum and AMAVS loading spectrum representative of Bomber-cargo-type maneuver spectrum. The specimens subjected to a constant amplitude loading and to A-10A loading spectra were made of 2024-T3XX aluminum alloy. The specimens subjected to AMAVS loading spectrum were made of 7075-T6XX aluminum alloy.

The test evaulation included examination of the crack growth data by constructing crack growth curves and fractographic examination using NDI equipment. The purpose of the fractographic examination was to determine the fracture surface characteristics, crack initiation sites, critical crack lengths, and modes of failure. The marker band cycles applied during the A-10A and AMAVS loading spectrum tests were used to reconstruct the growth curve, but in most cases it was extremely difficult to find every marker striation. The fracture surface marking associated with the loading spectrum is clearly indicated for specimen No. 63 (Figure 2.2). Note that the marking on the surface steadily widened until the crack approached the upstanding leg of the stringer, at which point the rate of growth slowed down substantially.

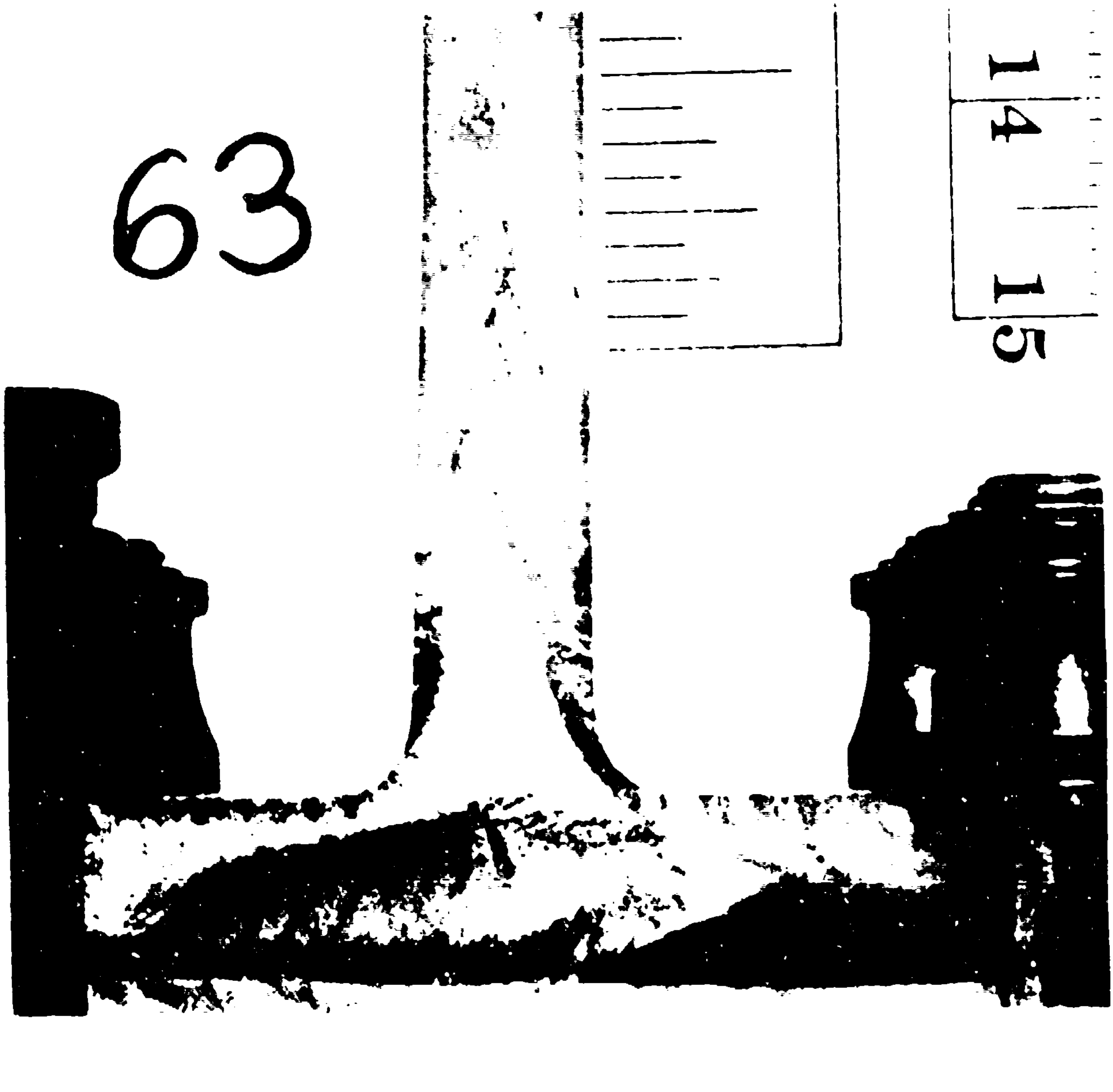

Figure 2.2. Fracture Surface of a Tee-Stringer Continuous Skin Subjected to AMAVS Loading Spectum

2.1.1 Lap-Joint Specimens Test Program

The test results of 36 lap-joint specimens were evaluated to determine the extent of crack initiation and crack growth. The lap-joint specimen configuration included single-shear lap-joint specimens and double-shear lap- joint specimens. The test matrix is shown in Table 2.1.

TABLE 2.1. LAP-JOINT SPECIMENS TEST MATRIX

GROUP	TYPE	MATERIAL FORM	SPECIMEN CONFIGURATION INTER-FER.	CLAMP-UP	SEALANT	APPLIED SPECTRUM	MAXIMUM STRESS (KSI)	AVERAGE CYCLES TO FAILURE
		2024-T3XX	No	No	No	C.A.	17.00	45,250
A	Single-Shear	2024-T3XX	No	No	No	A-10A	37.75	44,594
		7075-T6XX	No	No	No	AMAVS	37.75	5,387
		2024-T3XX	Yes	Yes	No	C.A.	17.00	96,700
B	Single-Shear	2024-T3XX	Yes	Yes	No	A-10A	37.75	59,798
		7075-T6XX	Yes	Yes	No	AMAVS	37.75	11,105
		2024-T3XX	Yes	Yes	Yes	C.A.	17.00	79,105
C	Single-Shear	2024-T3XX	Yes	Yes	Yes	A-10A	37.75	41,365
		7075-T6XX	Yes	Yes	Yes	AMAVS	37.75	9,980
		2024-T3XX	No	No	No	C.A.	13.1/4.7	214,050
A	Double-Shear	2024-T3XX	No	No	No	A-10A	37.75	39,185
		7075-T6XX	No	No	No	AMAVS	37.75	46,750
		2024-T3XX	Yes	Yes	No	C.A.	13.1/4.7	2×10^6
B	Double-Shear	2024-T3XX	Yes	Yes	No	A-10A	37.75	175,485
		7075-T6XX	Yes	Yes	No	AMAVS	37.75	148,917
		2024-T3XX	Yes	Yes	Yes	C.A.	13.1/4.7	129,300
C	Double-Shear	2024-T3XX	Yes	Yes	Yes	A-10A	37.75	107,038
		7075-T6XX	Yes	Yes	Yes	AMAVS	37.75	120,700

2.1.1.1 Single-Shear Lap-Joint Specimens Test Evaluation

The test results obtained from the single-shear lap-joint specimens lead to the following conclusions:

1) The fracture surface striations show crack growth approaching each other from adjacent holes. In most of the cases the size of the cracks were approximately the same, except the growth adjacent to the initial flaw

location was much larger. Crack initiation always occurred at the faying surface side of the specimens. In one case, (Group C specimen) the initiation occurred away from the hole.

2) Crack initiations of Group A specimens were the most widespread, followed by Groups B and C. Almost all holes across the fracture surface contained crack initiation, except those specimens subjected to AMAVS loading spectrum. The life-to-failure for those specimens was extremely low, mainly because of the relatively high stress level loading spectrum applied.

3) The highest number of cycles to failure were obtained from Group B specimens. The average improvements were approximately by factor of 2 with respect to Group A, and 20% with respect to Group C specimens.

4) Group C specimens had reduction in life due to the presence of sealant at the faying surface. The reductions in life were 22%, 44% and 11% for specimens subjected to a Constant Amplitude, A-10A and AMAVS Loading Spectrum, respectively.

2.1.1.2 Double-Shear Lap-Joint Specimens Test Evaluation

The test results obtained from the double-shear lap-joint specimens lead to the following conclusions;

1) Crack initiations were found mostly at holes adjacent to the initial flaw location. Little initiation was present at the other holes.

2) The extent of cracking was approximately the same for upper (head of Hi-Lok) and lower splice plates.

3) Crack shape was through the thickness, with tunneling in some cases.

4) Group B specimens exhibited the highest number of cycles-to-failure. For example, specimens subjected to A-10A loading spectrum with maximum gross stress of 37.5 Ksi, had a factor of 4.0 in life, compared with Group A specimens, and a factor of 1.65, compared with Group C specimens. Specimens subjected to constant amplitude loading with maximum stress of 13.1 Ksi failed at 214,000 cycles for Group A, and there was no failure at 2 X 10^6 cycles for Group B. The same trend followed for specimens subjected to AMAVS loading spectrum.

2.1.2 Stringer-Reinforced Specimens Test Program

The test results of 36 stringer-reinforced specimens were evaluated to determine the extend of crack initiation and crack growth. The stringer-reinforced specimens test matrix is presented in Table 2.2.

2.1.2.1 Stringer-Reinforced Specimens Test Evaluation

The test results obtained from the stringer-reinforced specimens lead to the following conclusions;

a) The majority of specimens exhibited early crack initiation. Exact time to initiation was difficult to determine. However, crack measurements during the test indicate early initiation at location diametrically opposite the initial flaw location (same hole).

b) Failure of stringer occurred just before, or at the same time that specimen failure occurred. Cracking in the skin was more extensive than in the stringers.

c) Of the 36 specimens tested, crack initiation diametrically opposite the initial flaw occurred in 34 cases.

d) Fifteen specimens out of twenty-four (excluding center L-stringers which contained only one fastener chord-wise) had initiation at a second hole prior to failure.

e) None of the four split skin specimens had initiation at a second hole, prior to failure.

f) The L-stringer specimens survived an average of 17 percent longer than the Tee-stringer specimens. This may be attributed to a relatively smaller ratio in cross-sectional area between the L-stringer/skin and the T-stringer/skin.

g) Over 75% of the specimens containing inside initial flaw survived longer than the specimens containing outside initial flaw. The life increase varied between 5% and 23%.

h) Similar specimen configurations tested at two stress levels and subjected to constant amplitude loading had an increase in life of a factor of 2 when the stress level was reduced by 25%.

i) There was 5% improvement in life for specimens with split skin compared to specimens with continuous skin.

Note that the hole with the initial flaw contained no interference fit fastener and no clamp-up. The adjacent fasteners had interference fit and clamp-up fasteners. There was no sealant at the faying surface.

TABLE 2.2. STRINGER-REINFORCED TEST MATRIX

SPECIMEN TYPE	FLAW CONFIGURATION	MATERIAL	APPLIED SPECTRUM	MAX STRESS (KSI)	AVERAGE CYCLES TO FAILURE
Center T-Stringer Continuous Skin	Inside (-1A)	2024-T3XX	A-10A	35.75	191,290
	Outside (-1B)	2024-T3XX	A-10A	35.75	202,143
Center L-Stringer Continuous Skin	Inside (-3A)	2024-T3XX	A-10A	35.75	240,210
	Outside (-3B)	2024-T3XX	A-10A	28.0	575,875
Edge L-Stringer Continuous Skin	Outside (-5A)	2024-T3XX	A-10A	35.75	130,860
	Inside (-5B)	2024-T3XX	A-10A	35.75	151,970
Center T-Stringer Continuous Skin	Inside (-1A)	2024-T3XX	C.A.	17.0/1.70	65,820
	Outside (-1B)	2024-T3XX	C.A.	17.0/1.70	65,140
Center L-Stringer Continuous Skin	Inside (-3A)	2024-T3XX	C.A.	17.0/1.70	76,025
	Outside (-3B)	2024-T3XX	C.A.	17.0/1.70	72,900
Edge L-Stringer Continuous Skin	Outside (-5A)	2024-T3XX	C.A.	17.0/1.70	67,136
	Inside (-5B)	2024-T3XX	C.A.	17.0/1.70	87,647
Center T-Stringer Continuous Skin	Inside (-7A)	2024-T3XX	AMAVS	30.0	146,742
	Outside (-7B)	2024-T3XX	AMAVS	30.0	180,150
Center L-Stringer Continuous Skin	Inside (-9A)	2024-T3XX	AMAVS	30.0	180,270
	Outside (-9B)	2024-T3XX	AMAVS	30.0	164,362
Edge L-Stringer Continuous Skin	Outside (-11A)	2024-T3XX	AMAVS	20.0	259,786
	Inside (-11B)	2024-T3XX	AMAVS	20.0	535,153

3.0 ANALYTICAL PREDICTIONS

The cycle-by-cycle crack growth method is most frequently used in predicting crack growth life. Because crack growth rates are sensitive to loading sequences, interaction models are necessary. The interaction models tend to slow the rate of growth subsequent to application of high load cycles, and accelerate the growth subsequent to compressive load application. Interaction models such as the Modified Willenborg have proved to be effective in most cases, but always require test verification. Another factor in predicting the crack growth life is the accuracy of the constant amplitude crack grcwth data. The Modified Walker equation which was used in this program, was constructed during Phase 1 of the program using Dog-Bone specimens. The Walker coefficients were derived for positive and negative stress ratios. However, crack growth rates at low-stress intensity are not always available. Extrapolation of the Walker's equation at this range may cause an error, usually on the conservative side. The majority of crack growth life occurs during the slow crack growth region. Unfortunately, the stress intensity solution for small cracks lacks the accuracy needed, especially when dealing with complex structures.

Two analytical methods were used during the course of crack growth life predictions. They included crack growth method 'Method 1' and combined method 'Method 2'. The crack growth method for continuing damage was consistent with the military design requirements specified in MIL-A-83444. The combined method for continuing damage is predicted using strain energy density as a parameter to govern the initiation at adjacent sites to the initial flaw. For the majority of the specimens, both analytical methods predicted lives on the conservative side. One exception is the predictions of single-shear lap-joint specimens subjected to AMAVS Loading Spectrum. For those specimens, the predicted life to failure was much higher than the test results. The results of the analytical prediction, using both methods, do not substantiate the effectiveness of one method vs. the other. However, the combined method predictions were superior to the crack growth method for predicting the continuing flaw location. Note that the combined method utilizes emperical data in predicting crack initiation. The accuracy of crack initiation is as good as the

accuracy of the various parameters and the scatter associated with them. For example, the parameter '$\alpha\beta\gamma$' which was supposed to differentiate between specimens of groups B and C, or specimens of group A (Ref. Table 2.1), was derived using a limited number of Dog-Bone-type specimens, and its accuracy is questionable. Other important parameters that determine crack initiation include damage index 'd_i' for constant amplitude loading spectrum and 'd_f' for variable amplitude loading spectrum. Other parameters used in the combined method predictions include the faying surface frictional forces, the clamp-up induced stresses about the hole boundaries, and the tilting effect of fasteners. All these parameters influence the crack growth life and should be evaluated thoroughly. In all test cases, the combined method predicted crack initiation to originate at the hole containing the initial flaw and on the diametrically opposite side. This was confirmed by the test results.

The percentage deviation between the experimental results and the analytical predictions for both methods are presented in Tables 2.3 and 2.4 for lap-joint specimens and stringer-reinforced specimens respectively. The percent deviation is defined in equation 2.1.

$$\%\ \text{DEV} = \frac{\text{LIFE (TEST)} - \text{LIFE (ANALYTICAL)}}{\text{LIFE (TEST)}} \quad \text{`0} \qquad (2.1)$$

The percent Deviation of the single-shear lap-joint specimens was 86.9% and 45.7% for Method 1 and Method 2, respectively. The percent deviation of the double-shear lap- joint specimens were 61.1% and 55.6% for Method 1 and Method 2, respectively. The overall percent deviation for the lap-joint specimens was 74.6% and 50% for Method 1 and Method 2, respectively. The overall percentage deviation of the stringer-reinforced specimens was 32.3% and 39.9% for Method 1 and Method 2, respectively.

Among all specimens tested, the best predicted lives were those which were subjected to a constant amplitude loading spectrum, followed by specimens subjected to A-10A and AMAVS loading spectrum. The worst predictions were the single-shear lap-joint specimens subjected to AMAVS loading spectrum.

TABLE 2-3. PERCENTAGE DEVIATION OF ANALYTICAL VS EXPERIMENTAL RESULTS OF LAP JOINT SPECIMENS

Specimen Configuration	Group	Applied Spectrum	Method 1 % Dev.	Method 2 % Dev.
Single-shear	A	C.A	9.9	32.5
	B	C.A.	46.2	30.0
	C	C.A.	49.2	41.8
	A	A-10A	45.2	66.2
	B	A-10A	59.2	11.1
	C	A-10A	40.1	50.5
	A	AMAVS	-310.0	- 69.5
	B	AMAVS	- 97.8	-110.0
Single-shear	C	AMAVS	-125.0	0.0
Double-shear	A	C.A.	43.4	46.0
	B	C.A.	N/A (1)	N/A (1)
	C	C.A.	83.9	80.3
	A	A-10A	18.6	42.7
	B	A-10A	81.8	19.5
	C	A-10A	70.2	71.7
	A	AMAVS	34.4	57.2
	B	AMAVS	79.4	47.6
Double-shear	C	AMAVS	74.6	71.9
		Overall % Deviation	74.6	49.9

(1) Specimens did not fail.

TABLE 2-4. PERCENTAGE DEVIATION OF ANALYTICAL VS EXPERIMENTAL RESULTS OF STRINGER-REINFORCED SPECIMENS

Specimen Type	Flaw Orientation	Applied Spectrum	Method 1 % Dev.	Method 2 % Dev.
Center T-Stringer	Inside	C.A.	14.6	9.6
	Outside	C.A.	11.1	25.3
Center L-Stringer	Inside	C.A.	15.8	19.9
	Outside	C.A.	12.2	16.5
Edge L-Stringer	Outside	C.A.	11.3	23.8
	Inside	C.A.	58.0	55.7
Center T-Stringer	Inside	A-10A	41.4	45.7
	Outside	A-10A	37.1	48.6
Center L-Stringer	Inside	A-10A	40.0	50.3
	Outside	A-10A	40.6	48.2
Edge L-Stringer	Outside	A-10A	8.8	28.0
	Inside	A-10A	51.0	50.7
Center T-Stringer	Inside	AMAVS	12.6	50.7
	Outside	AMAVS	40.2	46.8
Split Skin	Inside	AMAVS	70.1	65.9
	Outside	AMAVS	45.3	54.3
Edge L-Stringer	Outside	AMAVS	-8.2	-19.0
	Inside	AMAVS	62.6	60.0
	Overal % Deviation		32.3	39.9

4.0 GUIDELINES FOR IDENTIFYING CRITICAL LOCATION FOR DAMAGE TOLERANCE ANALYSIS

The process of selecting critical areas in a typical airframe structure is important for safety of flight and economic life considerations. The subject of structurally safe design has always been a top priority. Minimum weight, frequent inspection and repair, accessibility and inspectibility influence the economic life or durability of a structure. Efficient structural design is achieved through accurate and judicous engineering variation of these parameters. The selection of critical sections for damage tolerance is important to achieve these objectives. Because of the complexity of typical airframe structures, some of the "undesirable" design features find their way into the design. Structural features such as the splice of two elements with large amounts of load transfer, rapid change in cross section that may create build up in loads, open holes such as fuel transfer holes, and complex loading that follows unexpected secondary load paths may reduce the life substantially. The selection of critical sections for damage tolerance assessment should be based on a thorough evaluation of the stress environment and the geometrical configuration. The following guidelines are offered;

a) Evaluate stress environments, including primary and secondary load path. The tensile loads are always predominate, however, in some cases high compressive loads included in the loading spectrum may accelerate crack growth. Finite element modeling is helpful in predicting high stress concentration. However, deficiency in modeling may cause highly unconservative results.

b) Geometrical configuration may be critical. For example, high load transfer at a splice section is extremely damaging and should be treated as such.

c) Geometrical constraints such as closely spaced holes, proximity of holes to the edge of the part, and rapid change in cross-sectional area may cause reduction in crack growth life.

d) Redundancy in load path usually reduces the load concentration at the selected damage site. However, it may adversely effect the adjacent structure. For example, for a stringer to skin section, cracking in a stringer tend to increase the load in the adjacent skin, thus causing higher stresses and more possibilities of crack initiation and rapid growth.

e) The test program indicate beneficial effect due to fastener interference and, to a lesser degree, due to Hi-Lok clamp-up. However, a negative effect is concluded because of the presence of sealant at the faying surface. This may be attributed to the difference in coefficient of friction between surface with sealant to surface without sealant.

f) Environmental effects cause reduction in life. However, this subject is not addressed in this study.

5.0 RECOMMENDATIONS

Based upon the results of this study, the following recommendations are offered:

1) Continuing damage defined in MIL-A-83444 should be revised to reflect secondary crack initiation occurring diametrically opposite the primary flaw location. The exact time of introducing the secondary flaw may depend upon the structural configuration and the stress environment. However, it is safe to assume a secondary 0.005-in. corner flaw, when the primary flaw approaches '2D' from the center line of the hole. A schematic demonstration is shown in Figure 5.1.

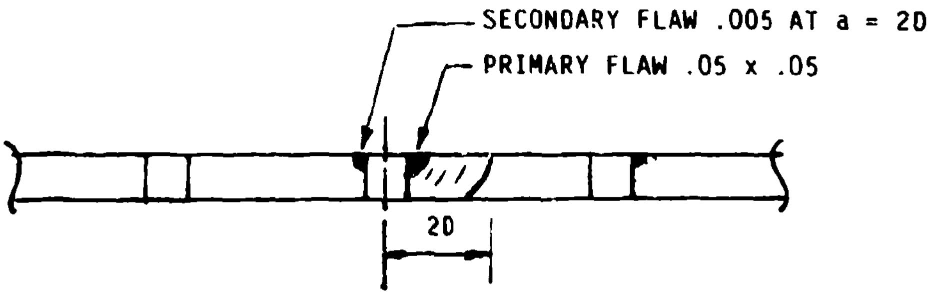

Figure 5.1. Secondary Flaw Assumption Recommendation

2) Aspect ratio of 0.5 - 0.75 for corner flaws at the edge of a hole at the time of break through thickness is more realistic than the current required by MIL-A-83444 of 1.0. An illustration is shown in Figure 5.2.

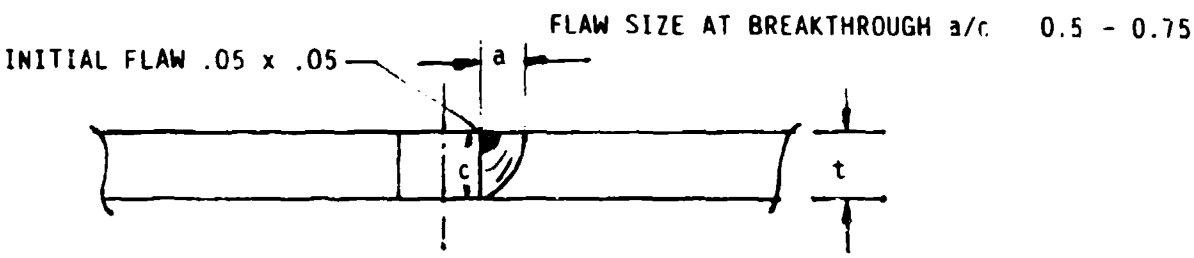

Figure 5.2. Aspect Ration of Flaw Recommendation

3) Constant amplitude crack growth rates should be developed at a low stress intensity factor of 3 - 5 Ksi $\sqrt{in.}$, or at crack growth rates of 10^{-8} in./cycle ; this will avoid the need of crack growth rate extrapolation which usually leads to conservative estimates. However, we found that in certain cases, unconservative extrapolation is possible.
4) For the majority of structural configurations the 'outside' initial flaw is more critical than the 'inside initial flaw' (Ref. Figure 2.1). However, local geometries should be carefully evaluated prior to initial flaw selection.
5) The combined method analysis is a powerful tool in determining crack initiation sites. However, empirical and analytical data of crack initiation should be investigated further. Dog-Bone type specimens are adequate for parameter evaluation. The proposed strain energy density governing crack initiation was found to be effective.
6) Interference fit fasteners offer the best degree of life enhancement for structures subjected to flight loads, and ought to be used whenever possible.
7) Single-shear lap-joint configuration should be avoided whenever it is possible. Double-shear lap-joint configuration is far superior.
8) The presence of sealant at the faying surface tends to decrease the crack growth life, and should be treated accordingly.
9) Marker band cycles are a useful tool in constructing crack growth curves subsequent to failure of a test specimen. However, identification of specific sequences against time is difficult. An alternative way would be the use of a variable band repeats application, in which the number of cycles in each application is distinctly different while the general characteristics of the "markers" are maintained.

5.1 FOLLOW-ON WORK

Crack initiation adjacent to the primary flaw may be predicted using the combined method. However, empirical parameters must be developed for representative geometric configuration and material form. The parameters α , β and γ were expected to determine the beneficial effect of interference fit, clamp-up and presence of sealant at the faying surfaces. However, crack initiation data

obtained during this program were not sufficient to characterize the influence of each parameter. It is, therefore, recommended that additional test programs be performed to substantiate these parameters. The test program should at least include the following:

a) Using standard crack initiation specimens, as shown in Vol. IV Figures 3-1 through 3-4, perform crack initiation test for the specimen configurations shown in Table 5.1. Two-hundred fifty-two specimens are recommended for test. Four specimens of each test are recommended, including the following permutations:
   - o Two material forms; 2024-T3XX and 7075-T6XX.
   - o Two specimen types: with one hole and with slotted hole (Ref. Vol. IV Figures 3-1 through 3-4).
   - o Two applied spectra: constant amplitude and variable amplitude loading.
   - o Two maximum stress levels; 28 Ksi and 20 Ksi.
   - o Four specimen configurations; open hole, 10%, 20% and 30% load transfer.

b) It is recommended that periodic NDI examinations be performed on the test specimens to determine exact time of initiation.

c) Following the test, the parameters α, β and γ should be evaluated using the strain energy method described in Phase 1 (Vol. II).

d) Using computer program 'DAMGRO', crack initiation should be predicted and correlations of experimental/analytical results should be performed.

e) Analytical prediction of 36 lap-joint specimens tested during Task IV should be updated if necessary.

f) The conclusions and recommendations as to the effectiveness of the combined method should be reviewed and updated as necessary.

TABLE 5.1. CRACK INITIATION SPECIMENS CONFIGURATION FOLLOW-ON WORK

GROUP	INTERFERENCE FIT	CLAMP-UP	SEALANT
A	No	No	No
B	Yes	No	No
C	No	Yes	No
D	No	No	Yes

☆ U.S. GOVERNMENT PRINTING OFFICE 1986 — 748-061/60505